A CFD Modeling of Oxy-coal Combustion and Sulfur Retention in a Circulating Fluidized Bed

Wu Zhou Changsui Zhao[*] *Lunbo Duan Xiaoping Chen*

School of Energy and Environment, Southeast University, Nanjing 210096, China

Corresponding author: Professor Changsui Zhao, +86-25-83793453 (tel. & fax), cszhao@seu.edu.cn

Abstracts Oxy-fuel circulating fluidized bed (CFB) combustion technology is one of the most prospective technologies for carbon capture and storage (CCS). Based on computational fluid dynamics (CFD) method, Euler-Euler model is employed to simulate the oxy-coal combustion processes in a 50kW CFB at Southeast University, China. The simulated processes during coal combustion include particle drying, raw coal devolatilization, volatile combustion, char combustion, char gasification and pollutants formation/reduction. Representative simulation results on hydrodynamics, combustion and pollutant emission characteristics are validated with experimental data in air and a good agreement is achieved.

Simulations are performed to investigate the effects of combustion atmospheres, including air (21%O_2/79%N_2) and oxygen/recycled flue gas (O_2/RFG) atmosphere with different O_2 concentration (from 21% to 40%). During combustion of Xuzhou bituminous coal in O_2/RFG modes with different O_2 concentrations, 70% volume fraction of CO_2 can be achieved with more than 25% volume fraction of H_2O. With the increase in O_2 inlet concentration, combustion efficiency is improved and gaseous pollutant SO_2 is enriched. The rates of char combustion and char gasification are compared in different atmospheres. Both indirect and direct sulphation mechanisms are considered and the corresponding reaction rates are calculated statistically.

Key words: CFD modeling; CFB; Oxy-coal combustion; Direct sulphation

INTRODUCTION

Oxy-fuel circulating fluidized bed (CFB) combustion technology is one of the most prospective technologies for carbon capture and storage (CCS)[1]. CFD modeling of gas-solid two-phase flow in CFB has already reached a high level[2] and oxygen-fired pulverized coal combustion is actively being investigated through CFD approach[3, 4], while numerical modeling of reactive multiphase flows in oxy-fired CFB is still in an early stage[5-7]. Our recent thorough literature review shows that multiphase CFD-based comprehensive models have not been widely adapted to circulating fluidized bed coal combustion processes in the open literature.

In this study, an Euler-Euler model using the Kinetic Theory of Granular Flow (KTGF) is employed to simulate the hydrodynamics of gas-solid flow in a CFB riser, coupled with heat transfer and chemical reaction sub-models. Gas-solid flow patterns, composition profiles of gas product and other important characteristics in a circulating fluidized bed coal combustor are predicted. Experimental data in air combustion are used to validate the model, and sulfur retention phenomena in different oxygen concentration are simulated.

MODEL DESCRIPTION

Detail descriptions of the 50kW CFB experimental system can be found in[8]. The simulated CFB riser configuration and detail dimensions are shown in Fig. 1 and mesh refinement near the inlet is displayed in Fig. 2. The riser is divided into the lower zone, middle zone and upper zone, with height of 0.8 m, 0.2 m

and 3.2 m, respectively. The coal inlet is located on the left side of the riser at the height of 0.7 m above the primary oxidant inlet. The solid recycle inlet, the secondary oxidant inlet and furnace outlet are located on the right side at 0.2 m, 0.9 m and 4.085 m, respectively. Based on computational fluid dynamics (CFD) method, a comprehensive dynamic 2D model is established to describe the coal combustion processes. The proximate and ultimate analyses of the coal tested are listed in Tab. 1.

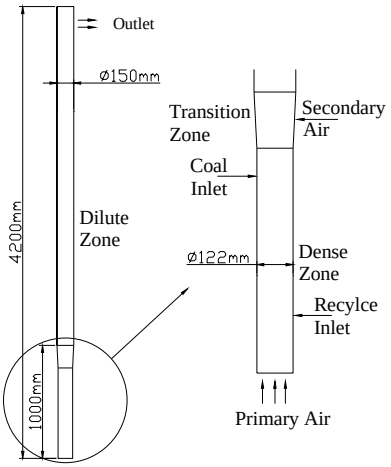

Fig. 1. Detail dimensions of the CFB riser

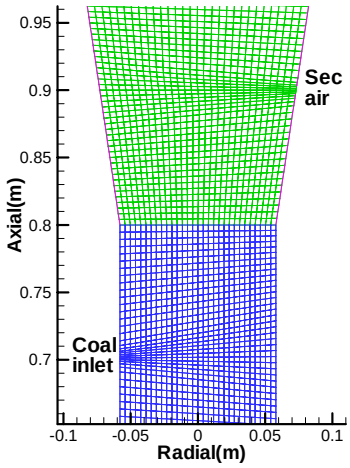

Fig. 2. Mesh refinement near the inlet

Tab. 1 Ultimate and proximate analyses of the coal

Sample	Ultimate analysis/ wt %					LHV	Proximate analysis/ wt %			
Xuzhou bituminous coal	C_{ad}	H_{ad}	O_{ad}	N_{ad}	S_{ad}	/ MJ/Kg	FC_{ad}	V_{ad}	A_{ad}	M_{ad}
	58.97	3.65	7.30	0.67	1.76	23.54	47.33	25.02	25.55	2.10

Main Assumptions

In order to decrease the impact of the strong nonlinear characteristic of the model and ensure the good convergence and acceptable computational time, the gas-solid hydrodynamic and coal combustion models are simplified as follows:

i) The simulation case is assumed as two-dimensional with the furnace depth of 0.1 m. The widths of dilute and dense zones in the 2-D simulation case are determined based on the corresponding cross-section area in the 3-D riser.

ii) O_2/N_2 or O_2/RFG mixture flows get into the CFB riser via the bottom or other inlets on it at uniform velocity. Gas density follows the incompressible ideal gas law.

iii) Particles are assumed isothermal, inelastic, smooth and monodispersed spheres.

iv) Small interaction forces such as lift force, thermophoretic force, Brownian force and virtual mass force are neglected. Energy transfer due to pressure stress work and viscous dissipation are not considered. Diffusion energy sources are excluded for good computational convergence.

Governing Equations

The conservation equations of mass, momentum, energy and species are applied to each phase (gas and solid). The standard κ-ε model is adopted to simulate the gas phase turbulence and KTGF for the solid phase. For the interphase momentum exchange coefficient, Wen and Yu drag model corrected by EMMS-Matrix[2] is compared with the Gidaspow[9] model. As part of the comprehensive model, the complicated processes of chemical reactions are considered by setting the source terms of mass, momentum, energy and/or species transport equations when the reactants are consumed and the products are created.

$$\frac{\partial}{\partial t}\left(\varepsilon_g \rho_g\right)+\nabla\cdot\left(\varepsilon_g \rho_g \vec{\upsilon}_g\right)=\dot{m}_{sg} \tag{1}$$

$$\frac{\partial}{\partial t}\left(\varepsilon_g \rho_g \vec{\upsilon}_g\right)+\nabla\cdot\left(\varepsilon_g \rho_g \vec{\upsilon}_g \vec{\upsilon}_g\right)=-\varepsilon_g \nabla p+\nabla\cdot\overline{\overline{\tau}}_g+\varepsilon_g \rho_g g+K_{sg}\left(\vec{\upsilon}_s-\vec{\upsilon}_g\right)+\dot{m}_{sg}\vec{\upsilon}_s \tag{2}$$

$$\frac{\partial}{\partial t}\left(\varepsilon_g \rho_g Y_i\right)+\nabla\cdot\left(\varepsilon_g \rho_g \vec{\upsilon}_g Y_i\right)=-\nabla\cdot\vec{J}_i+R_i \tag{3}$$

$$\frac{\partial}{\partial t}\left(\varepsilon_g \rho_g h_g\right)+\nabla\cdot\left(\varepsilon_g \rho_g \vec{\upsilon}_g h_g\right)=-\nabla\cdot\vec{q}_g+\alpha_{sg}\left(T_s-T_g\right)+S_g+\dot{m}_{sg}h_{sg} \tag{4}$$

ε , ρ, h and $\vec{\upsilon}$ are the volume fraction, the density, the enthalpy and the instantaneous velocity respectively of phase g, which stands for gas phase here. $\dot{m}_{sg}$ characterizes the mass transfer from solid phase to gas phase. p is pressure shared by all phases, $\overline{\overline{\tau}}_q$ is the stress-strain tensor, g is the gravity, $K_{sg}=K_{gs}$ is the interphase momentum exchange coefficient defined by EMMS-Matrix model. For the gas phase density, a mixture of incompressible ideal gas was assumed $\rho_g=\dfrac{p_{op}}{RT_g\sum_{i=1}^{n}\dfrac{Y_i}{w_i}}$, where p_{op},, T_g, Y_i and w_i are operation pressure, gas mixture mean temperature, mass fraction and the molecular weight for every species, respectively.

Chemical Reactions

The solid phase consists of 7 species (raw coal, water, char, calcium carbonate $CaCO_3$, calcium oxide CaO, calcium sulphate $CaSO_4$ and ash) and gas phase consists of 10 species (methane CH_4, oxygen O_2, carbon monoxide CO, carbon dioxide CO_2, water vapor H_2O, hydrogen H_2, tar, nitrogen monoxide NO, sulfur dioxide SO_2 and nitrogen N_2). Physical parameters of the mixtures obey the volume/mass-weighted-mixing law. The simulated processes during coal combustion include particle drying, raw coal devolatilization, volatile combustion, char combustion, char gasification and pollutants formation/reduction.

In the volatilization process, raw coal is consumed according to

$$1\,\text{rawcoal}\rightarrow Y_m\text{moisture}+Y_c\text{char}+Y_v\text{volatile}+(1-Y_m-Y_c-Y_v)\text{ash} \tag{R1}$$

The volatile matter consists of CH_4, CO, H_2O, CO_2, H_2 and tar, whose fraction compositions are determined from the Loison & Chauvin model[10]. The chemical formula of the tar is deduced combining with the proximate and ultimate analyses of the coal tested[11].

As homogeneous reactions (R2-R5), combustion of volatiles takes place once the volatiles escape from the raw coal particles. The char is consumed according to heterogeneous combustion (R6) and gasification (R7, R8) reactions. According to Field et al.[12], the char combustion rate is described by both the chemical kinetic reaction rate and the diffusion rate of oxygen to the particle surface and internal pores, which is widely used in fluidized bed combustion. The nitrogen and sulfur are partially released as tar and partially retained in the char during coal devolatilization. The nitrogen in the coal is considered to be partitioned between the volatiles and char such that its concentration in the volatiles is identical to that in the dry, ash-free parent coal. The sulfur is treated in the same way. With the combustion of tar and char, it is assumed that nitrogen and sulfur convert to NO and SO_2, respectively. Both indirect (R9, R10) and direct

(R11) desulfurization mechanisms are considered for SO_2 reduction. NO reductions are not included in this paper and will be considered in the future researches. Reaction rates information can be found in literatures[10, 13-16] and some are listed in Tab. 2.

$$CH_4 + 2O_2 \rightarrow CO_2 + 2H_2O \quad \text{(R2)}$$

$$CO + 1/2\,O_2 \rightarrow CO_2 \quad \text{(R3)}$$

$$H_2 + 1/2\,O_2 \rightarrow H_2O \quad \text{(R4)}$$

$$CH_{2.596}O_{0.158}N_{0.019}S_{0.021} + 1.600\,O_2 \rightarrow CO_2 + 1.298\,H_2O + 0.019\,NO + 0.021\,SO_2 \quad \text{(R5)}$$

$$C + 1/\Phi\,O_2 \rightarrow (2 - 2/\Phi)CO + (2/\Phi - 1)CO_2 \quad \text{(R6)}$$

$$C + CO_2 \rightarrow 2CO \quad \text{(R7)}$$

$$C + H_2O \rightarrow CO + H_2 \quad \text{(R8)}$$

$$CaCO_3 \rightarrow CaO + CO_2 \quad \text{(R9)}$$

$$CaO + SO_2 + 1/2\,O_2 \rightarrow CaSO_4 \quad \text{(R10)}$$

$$CaCO_3 + SO_2 + 1/2\,O_2 \rightarrow CaSO_4 + CO_2 \quad \text{(R11)}$$

Table 2: Reaction rates in the CFB riser

	Reaction rate (kmol/m^{3}s)	k
R9	$r_{10} = \frac{6(1-\varepsilon)\rho_s Y_{\mathrm{CaCO3}}}{d_p \rho_{\mathrm{CaCO3}}} \cdot k_{10} \frac{p_e - p_{CO2}}{p_e}$	$k_{10} = 1.01\times10^9 \exp(-2.05\times10^8/RT)$ [14]
		$p_e = 1.47\times10^{12} \exp(-1.613\times10^8 / RT)$
R10	$r_{11} = k_{11} Y_{\mathrm{CaO}} Y_{\mathrm{SO2}} \cdot (1-\varepsilon)\rho_s Y_{\mathrm{CaO}} s_g \cdot a$	$k_{11} = 490 \exp(-0.175\times10^8/RT)$ [16]
		$s_g = \begin{cases} -38.4\mathrm{T_s} + 5.6e4, \mathrm{T_s} \le 1253K \\ 35.9\mathrm{T_s} - 3.67\mathrm{e}4, \mathrm{T_s} > 1253K \end{cases}$ [a]
		$a = \exp\left(-571 \frac{C_{\mathrm{CaSO4}}}{(C_{\mathrm{CaCO3}} + C_{\mathrm{CaO}} + C_{\mathrm{CaSO4}}) MW_{\mathrm{CaCO3}}}\right)$
R11	$r_{12} = k_{12} C_{\mathrm{SO2}} \cdot (1-\varepsilon)\rho_s Y_{\mathrm{CaCO3}} s_g$	$k_{12} = 7.6 \exp(-0.8\times10^8/RT)$ [15]

a. Unit of specific surface area s_g is cm^2 g^{-1}.

Numerical Considerations

Parts of the initial and boundary conditions used in the simulation are listed in Tab. 3. The bed is initially filled with ash particles with static height of 0.4 m, where the volume fraction of the solids is 0.55. The maximum particle packing is limited to 0.63. The no-slip wall condition is used for the gas phase and partial-slip boundary condition for solid phase. The specific heat capacity of each gas species is calculated as a piecewise-linear function of temperature and viscosity as power law.

During the simulation, mass fractions of the solid species through the solid recycle inlet are set the same as outlet condition. To maintain constant bed inventory, mass flow rate of the recycled solid is adapted at real time combining with the mass flow rate of fed coal and outlet solid. Temperature of recycled solid is set to make sure that 30% of the thermal input is released along the dipleg and loopseal. For O_2/RFG cases, fuel feeding rate and O_2 supply rate are maintained the same. The volume fraction of O_2 in O_2/RFG oxidant is set to change from 21% to 40%. And fractions of other oxidant species are set by

calculating the flue gas compositions at real time with user-defined function codes compiled to the FLUENT software.

Table 3: Primary parameters used in simulations

Parameters	Value	Parameters	Value
Real density of char particles	1496 kg/m^3	Coal feed rate	8 kg/h
Real density of ash particles	2200 kg/m^3	Excess O_2 coefficient	1.2
Particle diameter	0.35 mm	Primary oxidant ratio	0.7
P-P restitution coefficient	0.9	Primary oxidant temperature	400 K
W-P restitution coefficient	0.95	Secondary oxidant temperature	298 K
Specularity coefficient	0.001	Heat loss through dilute zone wall	20%
Inlet coal temperature	298 K	Wall condition in the dense zone	Adiabatic
Initial temperature	1123 K	O_2/RFG volume fraction	21%/79%
O_2/N_2 volume fraction	21%/79%		30%/70%
			40%/60%

5 mm×5 mm grid is applied in the dense and transition zones and 8 mm×15 mm in the dilute zone. Mesh refinements near the inlets are applied with the total mesh number of nearly 8500. The time step is set as 1×10^{-4}. For the first 10 seconds, gas-ash fluidization is simulated at temperature of 1123 K without coal feeding, and then coal is continuously fed into the furnace. Flue gas recycling is executed from the fifteenth second. The simulation is conducted for 50 seconds and time-averaged distributions of flow and combustion characteristic variables are computed for the period from 30 s to 50 s.

RESULTS AND DISCUSSION

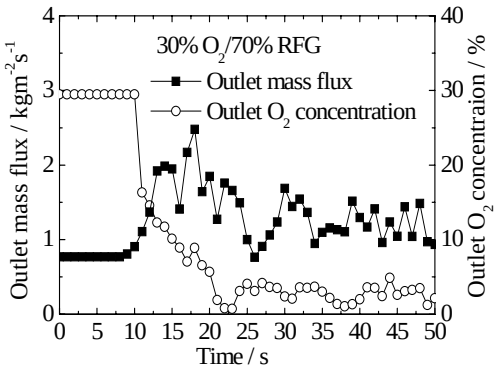

Fig. 3. Changes over time of monitored variables through the outlet during bituminous combustion in 30%O_2/70%RFG

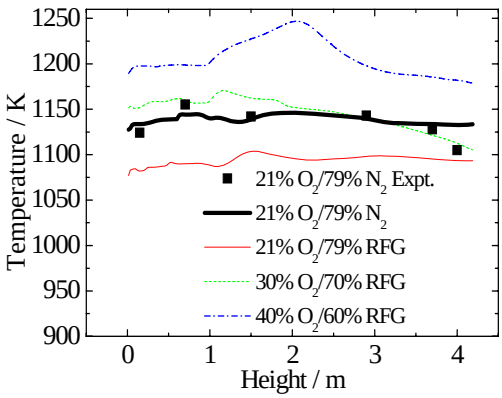

Fig. 4. Simulated axial distributions of cross-section averaged mixture temperature at the moment of 40 s among different atmospheres

Figure 3 shows the changes over time of mixture mass flux through the furnace outlet and O_2 concentration in the flue gas during bituminous coal combustion in 30%O_2/70%RFG atmosphere. They are monitored for the judgement of steady-state coal combustion processes. The same monitored variables are applied when dealing with other cases. It indicates that the time averaged variables computed from 30 s to 50 s are representative in description of primary characteristics in the real case.

Temperature Profiles

The simulated axial distributions of cross-section averaged mixture temperature at the moment of 40 s in different atmospheres are displayed in Fig. 4. Experimental data in air atmosphere are used to validate the model and a good agreement is achieved. For the same O_2 concentration, coal combustion under 21%O_2/79%RFG atmosphere yields the similar temperature trend to that in 21%O_2/79%N_2 with about 50 K lower. The reason is that water vapor and CO_2 have larger molar heat capacity than that of N_2. When firing in 30%O_2/70%RFG mixture, the bed temperature is slightly higher than that in air because of higher O_2 concentration. But temperature along the dilute zone decreases more obviously. That can be explained by the given certain amount of heat loss through the furnace wall in the upper dilute zone. Larger temperature decrease is yielded in lower volume gas flow because of lower particle concentration in the upper zone. A dramatic temperature rise and drop at the elevation of about 2 m in 40%O_2/60%RFG is observed, caused by over-fire volatile combustion and constant heat flux boundary condition, respectively. It indicates that the size distribution of bed materials plays an important role in controlling the furnace temperature. To avoid the phenomenon in 40%O_2/60%RFG mixture, bed materials with reasonable finer wide-size-distribution are required.

Composition Profiles

Fig. 5 plots contours of simulated distributions of gas compositions in the form of molar fraction at the moment of 40 s during bituminous combustion in 30% O_2/70% RFG combustion. There is an obvious lean O_2 zone near the coal feeding point due to the volatile and char combustion. The amount of CH_4 is very high near the coal feeding point as a result of devolatilization and then CH_4 concentration drops down immediately because of its combustion. Large amount of CH_4 combustion can be detected in the dilute zone. Since little $CaCO_3$ particles are elutriated to the dilute zone in the model, SO_2 concentration in the upper zone is higher. The cross-section temperature distribution is nearly uniform in the riser.

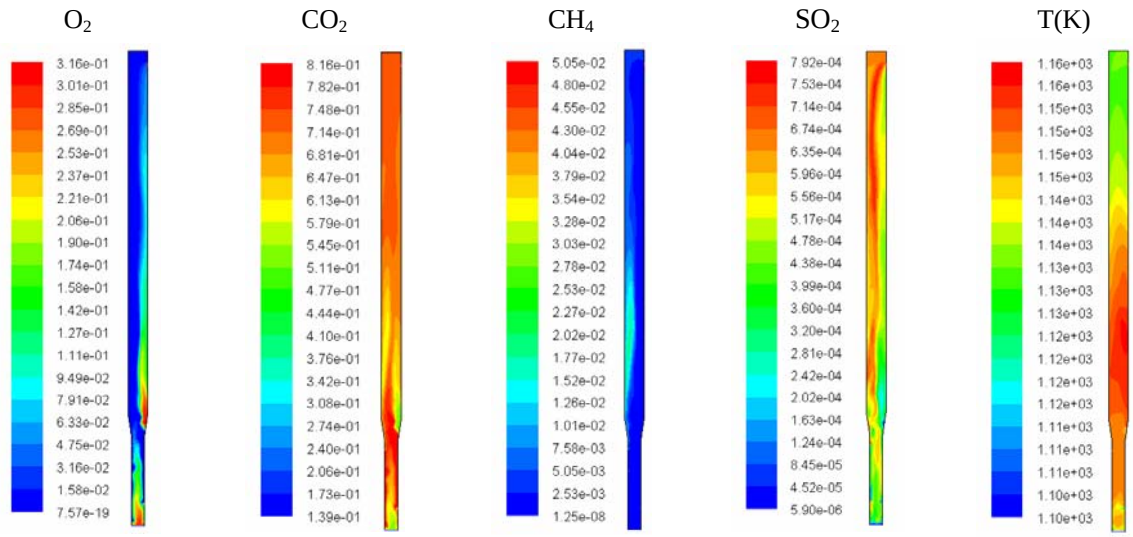

Fig. 5: Contours of transient molar fraction of gas components and temperature profile in 30%O_2/70%RFG

Figure 6 exhibits the simulated axial distributions of time and cross-section averaged mass fractions of gas components when firing in 30%O_2/70%RFG mixture. A large amount of O_2 is consumed in the dense zone and an increase in O_2 concentration is observed near the secondary oxidant injection location, while CO_2 concentration shows the opposite trend. The distributions in other cases behave in a similar way. The main components of the flue gas include CO_2 and H_2O, with CO_2 volume fraction of about 70% on wet basis, as shown in Fig. 7. 95% volume fraction of CO_2 can be achieved when calculating on dry basis. As the inlet O_2 concentration increases from 21% to 40%, outlet O_2 concentration increases accordingly in principle,

meanwhile more O_2 is consumed because of improved combustion efficiency, thus a minimum outlet O_2 concentration appears in the atmosphere near the 30% O_2/70% RFG.

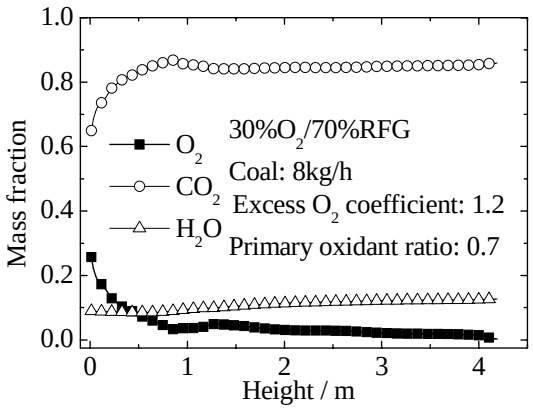

Fig. 6. Simulated axial distributions of time and cross-section averaged mass fractions of gas components during bituminous combustion in 30%O_2/70%RFG mixture

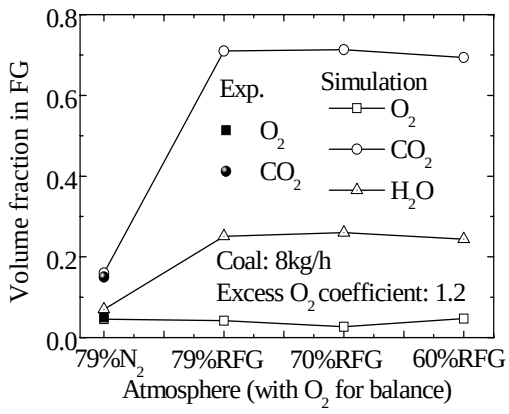

Fig. 7. Comparison of main components in the flue gas among different atmospheres during bituminous combustion

Pollutant emissions

For the sulfur retention model, self-desulphurization mechanism of coal ash is considered by specifying the mass fraction of $CaCO_3$ in the coal ash. It is obtained by XRF analysis of the coal ash. Limestone is also added to reduce more SO_2 emission. Figure 8 illustrates the SO_2 emissions under air combustion without considering self-desulphurization ability of coal, considering coal self-desulphurization ability and adding limestone. The results when considering self-desulphurization are in good agreement with the experiments. Figure 9 illustrates the SO_2 emissions under different atmospheres with or without adding limestone, considering self-desuphurization. The desulphurization efficiency under air achieves 92%, which is in a good agreement with experimental data. SO_2 is enriched as O_2 inlet concentration increases under O_2/RFG atmosphere.

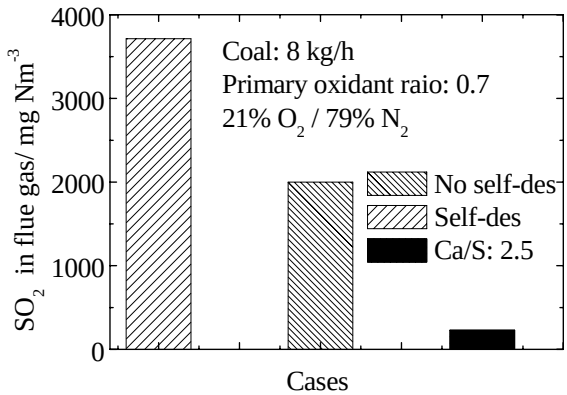

Fig. 8. Comparison of SO_2 emission considering different sulfur retention cases

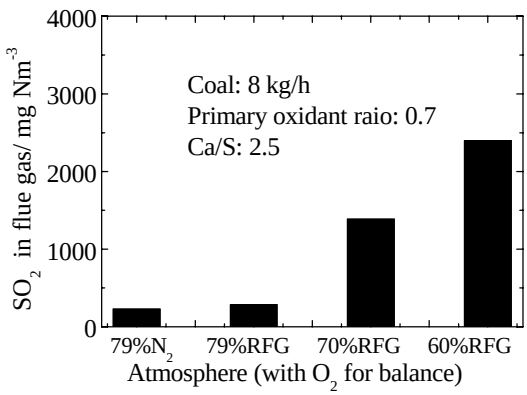

Fig. 9. Comparison of SO_2 emission under different atmospheres

Fig. 10 shows contours of transient molar concentration of solid components (CaO and $CaCO_3$) and reaction rate (Indirect desulphurization R10 and direct desulphurization R11) profiles in 30% O2/70% RFG combustion. The average molar concentrations of CaO and $CaCO_3$ in the riser are 0.017 and 0.011kmol/m^3, respectively. The average reaction rates of R10 and R11 are 7.9e-6 kmol/m^3s 5.3e-7 kmol/m^3s, respectively. That reveals 0.6 hour and 6 hours of full sulfation for the corresponding desulphurizer, which are consistent with the results reported by Borgwardt.[14]

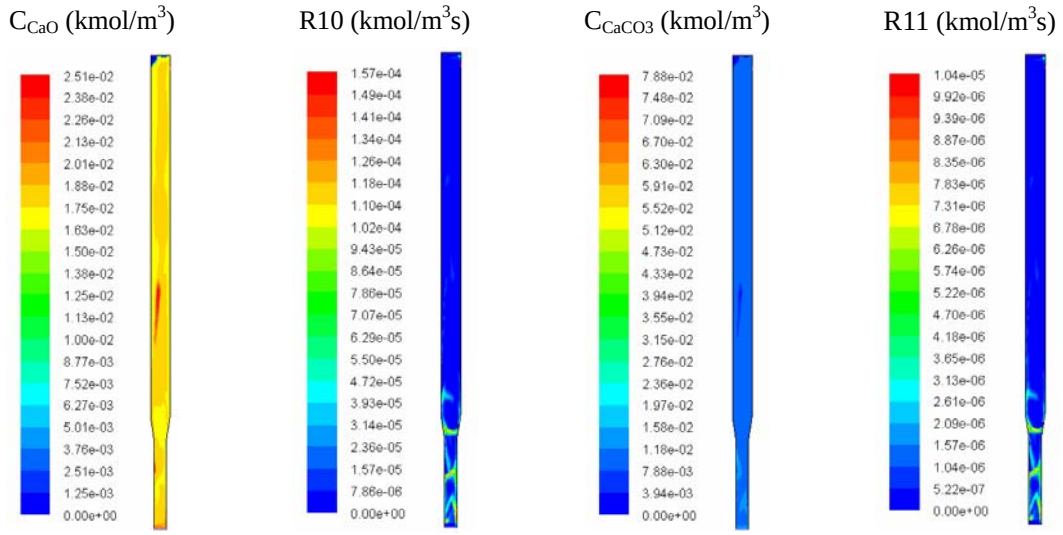

Fig. 10: Contours of transient molar concentration of solid components and reaction rate profiles in 30%O_2/70%RFG

CONCLUSIONS

A comprehensive coal combustion model in CFB based on Euler-Euler model was developed. Simulation results in 21% O_2/79% N_2 atmosphere were satisfactorily validated by the experimental data and a good agreement was achieved. For the interphase drag model, Wen and Yu model with EMMS/Matrix correction behaves better than Gidaspow model to predict the gas-solid flow in CFB combustor.

The flow behavior is obviously affected by the flue gas recycle ratio. Higher O_2 inlet concentration with smaller recycle ratio leads to lower volume gas flow and more dilute particle concentration in the upper zone. A certain higher O_2 inlet concentration will cause great drop in solid circulation rate and dramatic increase in furnace temperature. To avoid this phenomenon, bed materials with reasonable finer wide-size-distribution are required. Temperature results in this study also indicate that the one conservation equation of mixture energy is reliable for predicting the heat transfer characteristics in the CFB combustor.

When firing the Xuzhou bituminous coal in O_2/RFG mode, 70% volume fraction of CO_2 can be achieved with more than 25% volume fraction of H_2O in the flue gas. With the increase in O_2 inlet concentration, combustion efficiency is improved and gas pollutant SO_2 is enriched. Indirect and direct desulphurization models show consistent results with literature in sulfur retention.

ACKNOWLEDGEMENT

Financial supports of this work by the National Key Program of Basic Research of China (2006CB705806) and National Key Technology R&D Program (2006BAA03B02) are gratefully acknowledged.

REFERENCES

1. Wall TF. Combustion processes for carbon capture. Proceedings of the Combustion Institute. 2007;31:31-47.

2. Wang W, Lu B, Zhang N, Shi Z, Li J. A review of multiscale CFD for gas-solid CFB modeling. International Journal of Multiphase Flow. 2010;36:109-118.

3. Murphy JJ, Shaddix CR. Combustion kinetics of coal chars in oxygen-enriched environments. Combustion and Flame. 2006;144:710-729.

4. Tan Y, Croiset E, Douglas MA, Thambimuthu KV. Combustion characteristics of coal in a mixture of oxygen and recycled flue gas. Fuel. 2006;85:507-512.

5. Hartge E-U, Ratschow L, Wischnewski R, Werther J. CFD-simulation of a circulating fluidized bed riser. Particuology. 2009;7:283-296.

6. Krzywanski J, Czakiert T, Muskala W, Sekret R, Nowak W. Modeling of solid fuels combustion in

oxygen-enriched atmosphere in circulating fluidized bed boiler: Part 1. The mathematical model of fuel combustion in oxygen-enriched CFB environment. Fuel Processing Technology. 2010;91:290-295.
7. Krzywanski J, Czakiert T, Muskala W, Sekret R, Nowak W. Modeling of solid fuel combustion in oxygen-enriched atmosphere in circulating fluidized bed boiler: Part 2. Numerical simulations of heat transfer and gaseous pollutant emissions associated with coal combustion in O2/CO2 and O2/N2 atmospheres enriched with oxygen under circulating fluidized bed conditions. Fuel Processing Technology. 2010;91:364-368.
8. Zhou W, Zhao CS, Duan LB, Qu CR, Lu JY, Chen XP. Numerical simulation on hydrodynamics and combustion in a circulating fluidized bed under O2/CO2 and air atmospheres. 20th International Conference on Fluidized Bed Combustion, May 18, 2009 - May 21, 2009. 2009;883-888.
9. Gidaspow D, Jung J, Singh RK. Hydrodynamics of fluidization using kinetic theory: an emerging paradigm: 2002 Flour-Daniel lecture. Powder Technology. 2004;148:123-141.
10. Gungor A, Eskin N. Two-dimensional coal combustion modeling of CFB. International Journal of Thermal Sciences. 2008;47:157-174.
11. Duan L, Zhao C, Zhou W, Liang C, Chen X. Sulfur evolution from coal combustion in O2/CO2 mixture. Journal of Analytical and Applied Pyrolysis. 2009;86:269-273.
12. Field MA. Measurements of effect of rank on combustion rates of pulverized coal. Combustion and Flame. 1970;14:237-&.
13. Heikkinen JM, Venneker BCH, di Nola G, de Jong W, Spliethoff H. CFD simulation and experimental validation of co-combustion of chicken litter and MBM with pulverized coal in a flow reactor. Fuel Processing Technology. 2008;89:874-889.
14. Borgwardt RH, Bruce KR. Effect of specific surface area on the reactivity of CaO with SO2. Aiche Journal. 1986;32:239-246.
15. Snow MJH, Longwell JP, Sarofim AF. Direct sulfation of calcium-carbonate. Industrial & Engineering Chemistry Research. 1988;27:268-273.
16. Shuyan W, Lijie Y, Huilin L, Ding J, Yu L, Xiang L. Numerical analysis of particle clustering effects on desulphurization and NO emission in a circulating fluidized bed combustor. Fuel. 2008;87:870-877.